VDMA
Fluid Power Association

22nd ISC

# International Sealing Conference

**Stuttgart, Germany**
**October 01 - 02, 2024**

Sealing Technology –
Challenges accepted!

UNI STUTTGART

ISBN 978-3-8163-0768-6

Fachverband Fluidtechnik im VDMA e. V. Lyoner Str. 18
50628 Frankfurt am Main
Germany

Phone +49 69 6603-1513
E-Mail maximilian.baxmann@vdma.org
Internet www.vdma.org/fluid

# Development and testing of sleeve-type lip seals with stamped back-pumping structures

**Marco Gohs, Lothar Hörl, Frank Bauer**

The Back-Structured Shaft Seal (B3S) [1] was developed to achieve an optimal balance between static and dynamic tightness, thermal and chemical resistance, as well as high reliability and durability for PTFE shaft seals. Structures on the back of the sleeve create an active pumping mechanism in the sealing contact. This paper sums up the results of a stamped version in comparison to the laser engraved version. The stamping process causes significant alterations to the material properties of the seal. All prototypes underwent both static and dynamic tests which demonstrate that the B3S principle can be successfully implemented in a stamped version. However, the design of the structures must take additional influencing factors into account.

## 1 Introduction

In mechanical engineering, a multitude of diverse seals are employed to seal rotating shafts [2]. To guarantee a dependable, leakage-free seal, a back-pumping effect is indispensable. Consequently, shaft seals function as miniature pumps, actively pumping fluid back so that it does not occur as leakage. In the case of rotary shaft seals made of elastomer, a self-induced back-pumping effect is created by the geometry of the sealing edge and the surface roughness in contact with the shaft [3]. Therefore, no additional sealing aids are necessary [4].

In the event of high thermal or chemical loads, the use of elastomers is often no longer an option, necessitating the use of higher-grade materials such as PTFE compounds. Sleeve-type lip seals made of PTFE do not exhibit a self-induced back-pumping effect [5]. However, in order to achieve a back-pumping effect spiral grooves or other sealing aids in the sealing contact are used [6-7]. The back-structured shaft seal was developed at the Institute of Machine Components (IMA) for this purpose, representing an optimal combination of the positive properties of different shaft seal types. It ensures good static and dynamic tightness with high thermal and chemical resistance. The back-pumping effect is caused indirectly by structures on the backside of the sleeve, ensuring high reliability and a long service life [8].

This novel seal design was subjected to extensive testing and optimization with prototypes on test benches. The prototypes for this were produced by laser engraving. In order to facilitate more efficient production with reduced emissions, particularly in view of possible restrictions in the use of per- and polyfluoroalkyl substances (PFAS), stamping has now been tested as an alternative production process. Compared to laser engraving, stamping results in additional alterations to the material properties and thus a change in the sealing properties. The same geometry as a pumping structure exhibits different properties in stamped form than in laser engraved form. This paper therefore compares the functional behavior of stamped back-structured shaft seals to that of the laser engraved reference variant. The advantages and special features of the stamped variant are demonstrated on the basis of experimental investigations, thereby illustrating the suitability of stamping as an alternative manufacturing process for back-structured shaft seals.

## 2 Sleeve type lip seals made of PTFE

PTFE is utilized in the production of sleeve type lip seals, which is compounded with fillers to reduce wear and creep tendency while maintaining high chemical and thermal resistance and optimum dry-running properties [9]. Flat disks are typically employed, which are clamped in sheet metal rings. Due to the inner diameter being smaller than the shaft diameter, the sleeve lies flat on the shaft surface after the installation, as illustrated in Figure 1. Due to the surface roughness and the lack of a back-pumping effect, it is inevitable that leakage will occur during operation.

Spiral grooves (Figure 1, middle) or stamped structures in the sealing contact (Figure 1, right) are used to enhance dynamic tightness. However, the continuous spiral reduces static tightness and only one direction of rotation is possible [7]. Stamped structures in the sealing contact can also be utilized for shafts rotating in both directions, but are subject to heavy wear and are therefore not durable [6,10]. Bidirectional hydrodynamic seals where first mentioned in [11].

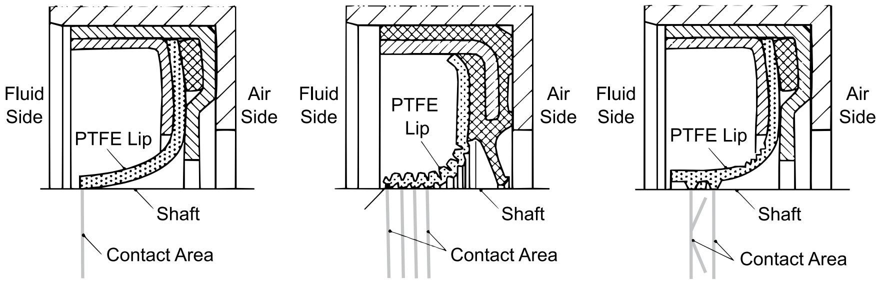


*Figure 1: PTFE Lip Seals without and with Sealing Aids [8]*

### 2.1 Back Structured Shaft Seal

The indirect structuring of the B3S combines the advantages of the three aforementioned variants. As the structures are not in the sealing contact, the static tightness remains at a similarly high level as with the unstructured sleeve type lip seal. The structures are applied as indentations on the side facing away from the shaft. As a result of the widening of the inner diameter during assembly, flat, very active pumping channels result in the contact area, as illustrated in Figure 2. The geometry of the structuring allows for the creation of channels with a wide range of shapes, enabling the realization of both unidirectional and bidirectional structures [12]. The active pumping channels in the sealing contact are a consequence of the structuring on the backside and remain effective even in the presence of wear, as they are also activated in dynamic operation by drag pressure due to the locally lower stiffness of the material.

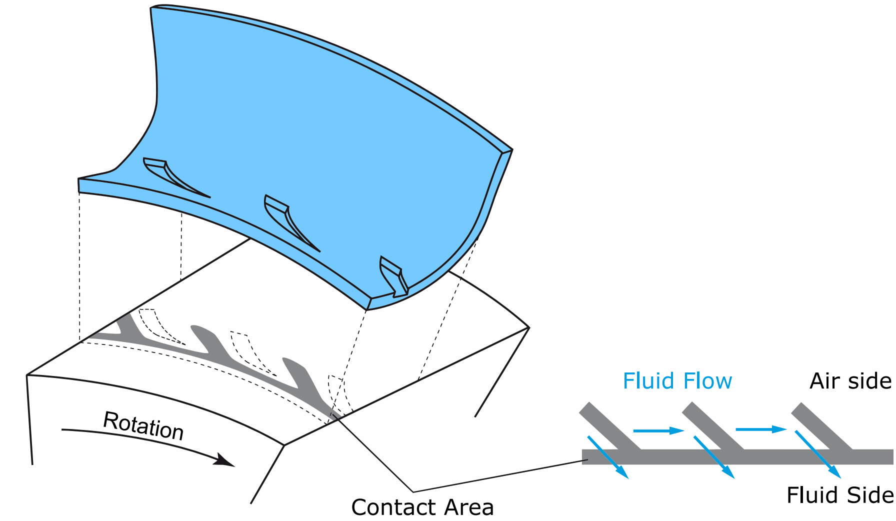


*Figure 2: Working Principle of the Back Structured Shaft Seal [12]*

A comprehensive account of the B3S's functionality and testing on laser engraved variants has been previously published by STOLL and DAKOV [8,12]. Optimal geometries were developed and tested for various applications using different geometry variants. The sickle-shaped geometry implemented here was found to be the most robust variant. In particular, the position, number, and depth of the structures can be varied within certain limits without a significant impact on the function. This allows for a seamless transition to a stamping die.

## 3 Manufacturing of the Prototypes

The raw material utilized in the production of the sheet material is a PTFE compound filled with glass spheres [13]. The base material in this case is expanded PTFE, which exhibits compressibility and provides optimal conditions for the stamping process. The same raw material was employed in the experiments before with the laser engraved variant, ensuring direct comparability with previous investigations.

### 3.1 The Stamping Process

For the production of stamped back-structured shaft seals, the geometry was first adapted to the requirements of a stamping die. Prototypes were then produced and the influence of the stamping parameters, namely pressure, duration and temperature during stamping, was investigated.

### 3.2 Adaptation of the geometry

A subtractive manufacturing process, such as laser engraving, allows for the creation of structures with no restrictions on distance, geometry, or depth. This enables the structuring to be designed with great freedom, with the goal of achieving the optimal pumping effect. However, material deposition during stamping is necessary, and there must be sufficient distance between structures to ensure clean impression accuracy. Additionally, it is essential to ensure that the metal stamping die, which is to be produced as a negative of the stamped geometry, can be manufactured. The optimized geometry of the laser engraved version (Figure 3, left) was therefore adapted (Figure 3, right). In order to achieve a greater distance between the structures, the number of structures was reduced and the shape slightly adjusted.

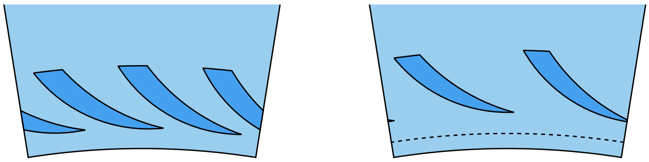

*Figure 3: Reference Geometry and for Stamping optimized Version*

The inner diameter was chosen slightly smaller to allow cutting to obtain an optimal edge. This is done by removing the burr caused by the gap of the die. The dotted line marks the position where the cut is made.

### 3.3 The Stamping Process

The prototypes were produced on a stamping press with heatable plates, as illustrated in Figure 4. For this purpose, the disk of raw material is placed between a milled stamping die, which has the shape of the structuring as a negative on the surface, and a counter mold. The heatable plates at the top and bottom can heat the stamping die and the disk up to 270°C. The stamping process is realized via a pressure-controlled hydraulic cylinder. It can be subjected to a pressure of up to 25MPa, which corresponds to a force of up to 200kN. The PTFE disks have an inner diameter of 65mm and an outer diameter of 100mm.

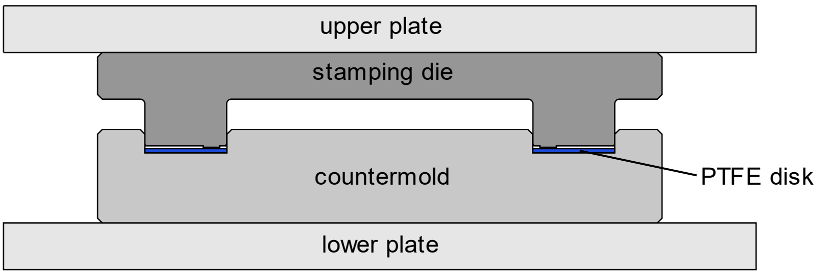


*Figure 4: Scheme of the Stamping Process*

The stamping process can be divided into four steps. First, the disk is placed in the die. Second, the die is heated for approximately 10 minutes between the preheated plates of the press. After heating, pressure is applied and maintained for a predetermined time. For all the variants in this paper the pressure was applied for one minute. Finally, the stamped disk is removed and allowed to cool down. The stamping die used for the prototypes is shown in Figure 5.

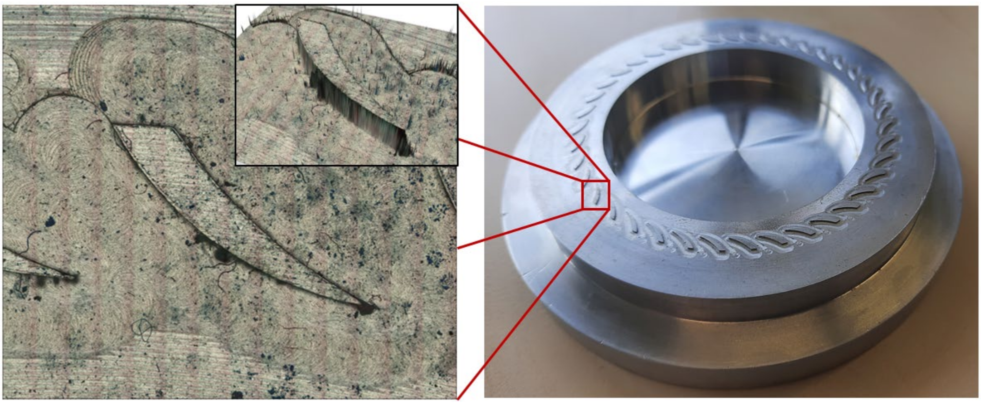

*Figure 5: Stamping Die*

The structures of the die have an average height of approximately 0.32 mm.

### 3.4 Evaluation of the structures

Different stamping parameters result in variations in the replication of the stamping die in the material to be stamped. They also cause shallow indentations on the opposing sleeve surface. The variants enumerated in Table 1 were created with the objective of identifying the relationships between the stamping parameters and the resulting stamped geometry. The mean contact pressure in table 1 is the mean pressure applied on the whole disk surface during the stamping process.

*Table 1: Stamping Parameters of the Analyzed Variants*

| Stamping Pressure | | 20 MPa | 10 MPa | 5 MPa | 2.5 MPa |
|---|---|---|---|---|---|
| Mean Contact Pressure | | 35.3 MPa | 17.6 MPa | 8.8 MPa | 4.4 MPa |
| Stamping Temperature | 20°C | G001 | G002 | G003 | G004 |
| | 200°C | G005 | G006 | G007 | G008 |

Figure 6 illustrates the three variants G001, G004 and G005. The differences in characteristics between the structures with varying stamping parameters are clearly evident.

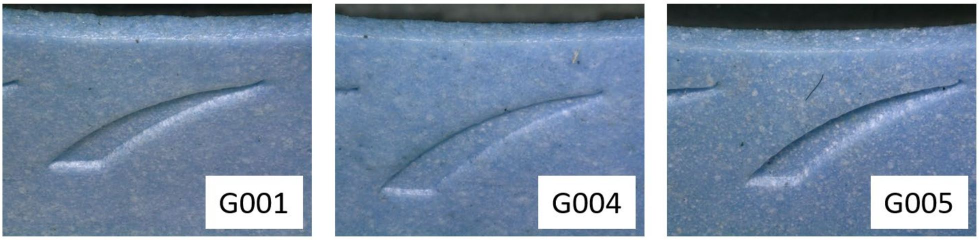


*Figure 6: Examples of Stamped Structures with different Stamping Parameters*

The depth of the structures and the depth of the indentations in the contact area were measured and evaluated. The surface measurements were conducted on a laser scanning microscope (Keyence VK9700 Gen. II). An illustrative example of a measurement of the top and bottom sides is presented in Figure 7.

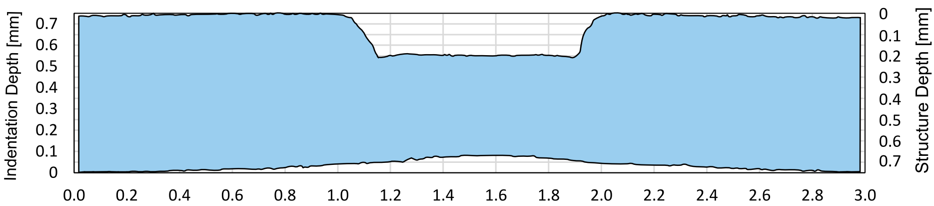


*Figure 7: Example of a Measurement of the Top and Bottom Side*

### 3.4.1 Structures on the back

Figure 8 presents the measured depths of the various variants.

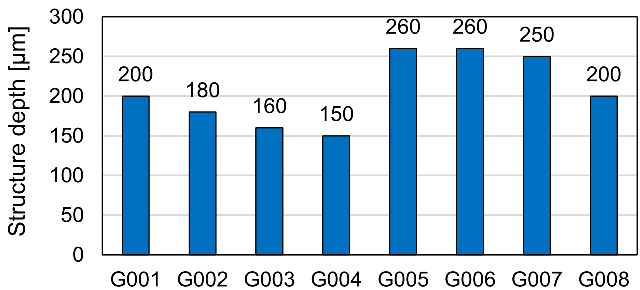


*Figure 8: Depth of the Stamped Structures*

The structures of the variants stamped at 200°C are significantly deeper than those of the variants stamped at 20°C. This behavior can be explained by the fact that the PTFE flows more strongly at higher temperatures and already deforms plastically at lower strains. The structure depth decreases with lower stamping pressure. In the variant stamped at 200°C, no discernible differences in depth are observed between 10 and 20MPa stamping pressure. Therefore, 10MPa at 200°C is sufficient for achieving the maximum depth of the structure.

The stamping temperature also has a significant effect on the shape of the stamped structure. Figure 9 shows the cross-sectional geometry of a structure stamped at 20°C (left) and one stamped at 200°C (right). Note that the structures stamped at higher temperature have significantly sharper edges. The structures stamped at 20°C show a curvature of the bottom surface in addition to the strongly rounded top edges.

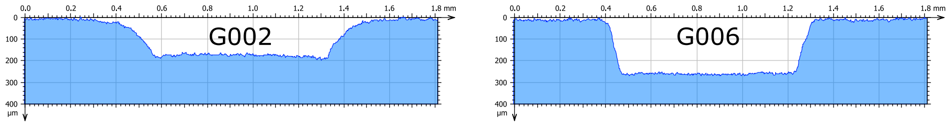


*Figure 9: Profiles of the Stamped Structures at different Temperatures*

### 3.4.2 Structures in the contact area

The indentations that have been formed on the opposite surface are approximately 50 µm deep at the deepest point in the variant stamped at 200°C. In the variant stamped at 20°C, they are slightly deeper at approximately 80 µm. The results from the contact analysis, which follow in section 4.2.2, also confirm this.

In conclusion, it can be stated that a higher stamping temperature results in deeper structures on the back side and a more accurate geometry of the structures. Conversely, a higher stamping temperature results in shallower indentations on the contact side.

## 4 Experimental tests of the functionality

In order to demonstrate the effect of the stamped structures and to compare them with the laser engraved version, a series of static and dynamic tests were carried out on prototypes.

### 4.1 Manufacturing and selection of variants

Prototypes were produced with the following stamping parameters for the purpose of experimental investigation of the stamped variant:

- **S01**: 1 minute at 200°C and 20MPa stamping pressure
- **S02**: 1 minute at 20°C and 20MPa stamping pressure

In addition to a variant without pumping structures, two reference variants were produced with laser engraving to permit a direct comparison under identical test conditions:

- **WS**: Smooth lip without pumping structures
- **L01**: Reference geometry with 60 structures, 0,4mm deep
- **L02**: Geometry of the stamped variant with 40 structures, 0,25mm deep

A series of four identical seals of each variant were tested in order to ascertain the impact of the stamping process. The reference variant, L01, corresponds to the unchanged original laser engraved variant. The variant L02 was equipped with the geometry adapted for the stamping die. A depth of 0.25 mm was selected, as this corresponds to the measured structure depth of the stamped variants. L02 therefore represents the geometrically identical equivalent to the stamped variants. Due to the laser engraving process, this variant does not exhibit the material-related changes caused by the stamping process. Consequently, it is possible to differentiate the properties caused by the structure from those caused by the stamping process.

### 4.2 Preliminary and follow-up studies

The radial load was quantified on all manufactured variants both before and after the tests. Furthermore, the contact area was evaluated, and the sealing edges were visually inspected.

#### 4.2.1 Radial load

In the case of seals, the radial load is the load with which the sealing edge is pressed against the shaft. The measurements were conducted on a radial load measuring device using the split shaft method and Automatic Diameter Control [14]. The sealing rings were mounted on a shaft and stored for one hour prior to the first measurement. The second measurement was conducted after the static test. This corresponds to a total time of approximately 240 hours mounted on the shaft at 20°C. The third measurement was conducted after the subsequent endurance test. The seals were therefore mounted on the shaft for a total of approximately 480 hours and exposed to an oil temperature of 20°C for half the time and 120°C for the other half. The measured values are presented in Figure 10. For each variant, all the seals were measured at four points, with each point offset by 90°. Consequently, each bar is averaged over a total of 16 values.

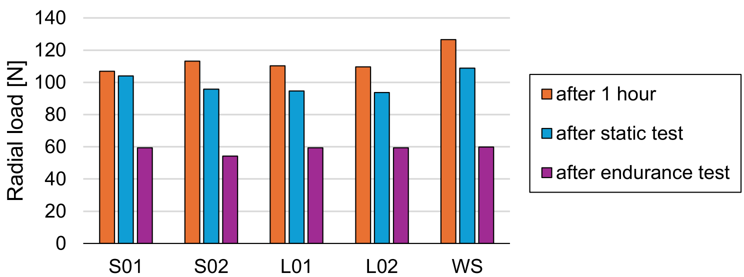


*Figure 10: Radial Loads*

It is clear that the stamping process of version S01 and S02 has an effect on the radial load compared to the smooth lip WS. The smooth lip WS also represents the values of the disk before the stamping process as it is not possible to measure the radial load before and after the stamping process on the same seal due to plastic deformations while mounting. The radial load after 1 hour is slightly lower for the variant S01 than for the variant S02. However, with increasing storage time on the shaft, the radial loads of the variant S01 remain almost constant, while the radial load of the variants S02 decreases significantly. The behavior of the stamped variants S01 and S02 is very similar to the behavior of the laser engraved variants L01 and L02. After 240 hours of continuous running at 120°C, the radial loads are almost identical for all variants. However, they remain significantly lower than before the endurance test.

### 4.2.2 Contact analysis

During contact analysis, the seals are mounted on a hollow glass shaft that is illuminated from the front surface. This type of illumination makes the areas that touch the shaft appear bright, which allows for the visualization of the very flat structures in the sealing contact. The images were taken with a Sealobserver, which enables the observation of the sealing edge radially from the inside to the outside through the glass shaft onto the sealing edge [15]. Selected images of the different variants before the tests are shown in Figure 11.

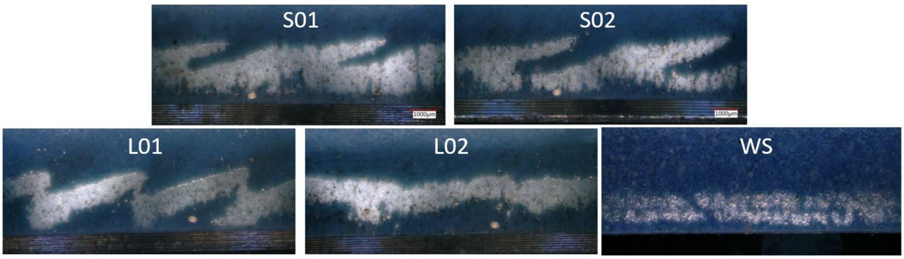


*Figure 11: Contact Areas before the Endurance Test*

It is evident that both stamped variants exhibit a continuous pressure line on the fluid side in the circumferential direction. This renders the stamped variant more advantageous in this regard than the reference variant L01. The laser engraved variant L02 clearly demonstrates that, in the absence of the additional effects resulting from the stamping process, the structuring merely creates a relatively weak pumping structure in the form of a wavy pressure line and lacks any ridges in the pressure distribution.

The contact analysis after the endurance test at 120°C in Figure 12 shows that the laser engraved structures have become less pronounced. In the stamped variants, there is a clear difference between the variants S01 and S02 visible. In variant S01, the channels have even become slightly more pronounced, while in variant S02, the geometry of the channels has changed significantly. This again illustrates the influence of the stamping parameters on the back-pumping structures.

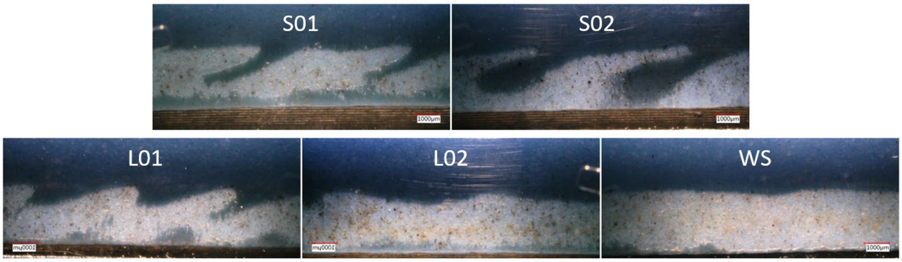


*Figure 12: Contact Areas after the Endurance Test*

## 4.3 Static tightness

In the process of testing the static tightness, the seal is completely flooded on the fluid side and the extent of the leakage at the sealing edge is evaluated visually. This evaluation is carried out at specified intervals. The leakage is qualitatively divided into six classes, which are illustrated in Figure 13. The classes range from P6, which indicates that no leakage is visible, to P1, which signifies that the leakage has already reached the housing. The classes in between are used for finer gradation. The ratings of the five variants are presented in Figure 13.

| Duration | Variant | | | | |
|---|---|---|---|---|---|
| | S01 | S02 | WS | L01 | L02 |
| 0 min | P6 | P6 | P6 | P6 | P6 |
| 5 min | P6 | P6 | P6 | P6 | P6 |
| 30 min | P6 | P5 | P6 | P6 | P6 |
| 1 h | P6 | P5 | P6 | P6 | P6 |
| 3 h | P6 | P5 | P6 | P5 | P6 |
| 6 h | P6 | P4 | P6 | P5 | P6 |
| 12 h | P5 | P3 | P6 | P4 | P6 |
| 24 h | P5 | P2 | P6 | P4 | P6 |
| 48 h | P5 | P2 | P6 | P3 | P5 |
| 72 h | P5 | P1 | P5 | P2 | P5 |
| 96 h | P4 | P1 | P5 | P2 | P5 |
| 168 h | P4 | P1 | P5 | P1 | P5 |
| 192 h | P3 | P1 | P4 | P1 | P4 |

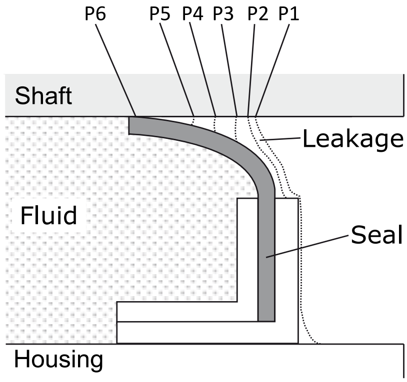


*Figure 13: Static Leakage and Measurement Method [7]*

As anticipated, the variant WS without any structuring (WS) exhibited the best performance. The variant L02 with the laser engraved equivalent structures exhibited slightly inferior performance, but within a similar order of magnitude. The at 200°C stamped variants (S01) exhibited particularly favorable results, demonstrating significantly enhanced static tightness compared to the reference structure (L01) despite the channels that are clearly visible in the contact analysis. This evidence demonstrates the significance of the closed pressure line on the fluid side, which is absent in the laser engraved reference variant (L01) and consequently results in inferior static tightness.

## 4.4 Pumping rates

To test the pumping rate, the seals are mounted on the test bench in reverse. Fluid is now present on the air side and the pumping action pumps fluid from the air side to the fluid side of the seal. With the fluid side now facing outward, the amount of pumped fluid escapes and can be measured. Pumping rate measurements were taken both before and after the endurance test on two samples of each version to evaluate the change in pumping efficiency over time. Figure 14 shows the measured pumping rates before the endurance test and Figure 15 shows the values after the endurance test.

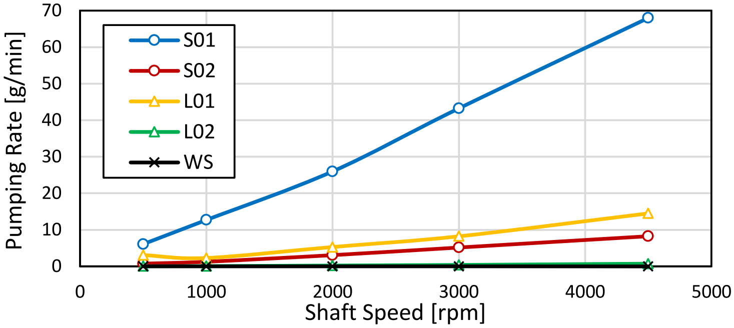


*Figure 14: Pumping Rates before the Endurance Test*

As expected, the seals without pumping structures (WS) also show no pumping effect. The laser engraved reference variant L01 has a pumping rate of about 15 g/min at 4500 rpm. The two stamped variants S01 and S02 differ significantly. The variant S01 had more than four times the pumping rate of the laser engraved reference variant L01. However, variant S02 had a lower pumping rate than the reference variant L01. Variant L02 clearly shows that the structuring of the stamped versions alone, without the influence of the stamping process, has a very low pumping rate. It can be concluded that the very good pumping effect is mainly caused by the changes that occur during the stamping process, in particular the significantly reinforced structures in the sealing contact.

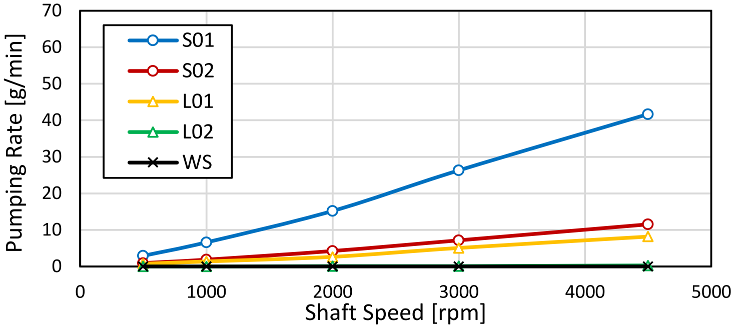


*Figure 15: Pumping Rates after the Endurance Test*

As a result of the endurance test, the pumping effect of the laser engraved variants L01 and L02 and the stamped variant S01 is reduced by more than 30%. The stamped variant LS02 shows a slight improvement in the pumping effect, which means that both stamped variants now have a higher pumping effect than the laser engraved variants. It is positive to emphasize that all back-structured variants show a clear pumping effect even after the endurance test, thus demonstrating the durability of the structuring.

### 4.5 Endurance test

Endurance tests were performed to verify the function over a longer period of use. The test conditions and a section of the used test rig are shown in Figure 16.


| | |
|---|---|
| Shaft Diameter | 80 mm |
| Shaft Material | 100Cr6 |
| Surface | Plunge Ground |
| Oil | 0W 30 |
| Oil Temperature | 120 °C |
| Oil Level | Shaft Centre |
| Speed | 4,500 rpm |
| Duration | 240 h |

*Figure 16: Test Rig and Operation Conditions*

None of the stamped variants showed any leakage over the entire test period. The exceptions were individual failures that were due to other causes and therefore could not be included in the evaluation of the stamped structure.

## 5 Influence on the material behavior through the stamping process

The PTFE compound used is compressible, which alters the mechanical properties as a consequence of the stamping process. To ascertain the influence of this phenomenon, tensile tests were conducted on compressed raw material at 20°C and 120°C. The raw material was therefore pressed at 20°C and 200°C. The tensile specimens were then punched out of the prepared material and the thickness was measured, (Figure 17 left). The material compressed at 20°C exhibited a compression of approximately 13%, while the material compressed at 200°C showed a compression of around 46%.

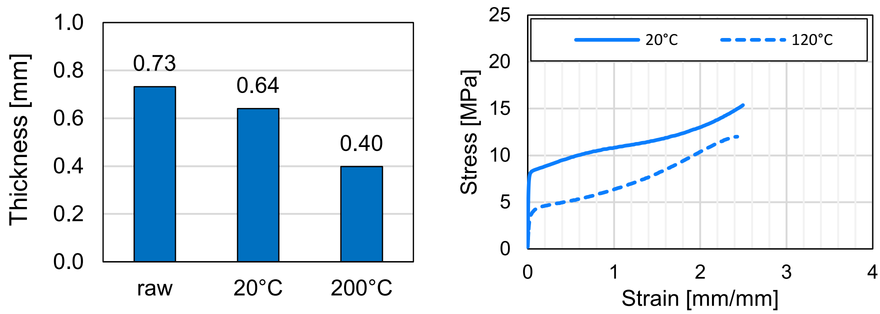


*Figure 17: Measured Specimen Thickness and Stress-Strain Curve of the Raw Material*

Figure 17 on the right shows the stress-strain curves of the raw material measured at 20°C and 120°C. The stress is reduced by about 50% due to the increased ambient temperature whereas the elongation at break remains nearly the same at about 2.5 mm/mm.

The stress-strain curves of the compressed PTFE sheets are shown in Figure 18. The plot on the left shows measurements on specimens compressed at 20°C for one and ten minutes and the plot on the right shows the measurements on specimens compressed at 200°C for one minute.

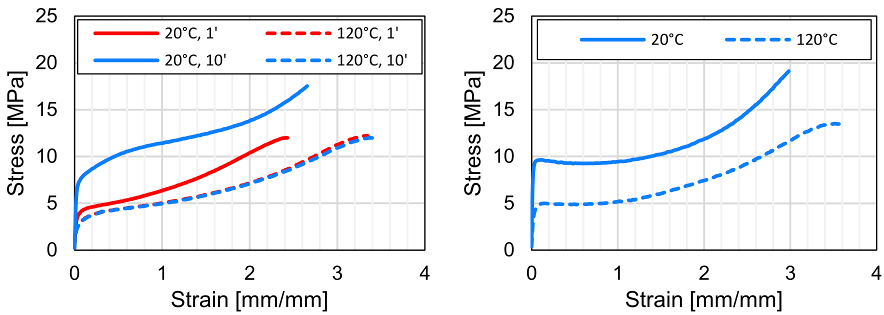


*Figure 18: Stress-Strain Curves of the Compressed Material at 20°C and 200°C*

At 20°C it is evident that the length of time the material has been compressed has a significant influence on the stress-strain behavior. The material compressed for 10 minutes almost reaches the values of the raw material, while the material compressed for one minute shows significantly lower stresses. This difference is not visible in the tensile tests at 120°C. It can therefore be concluded that the residual stresses generated by the pressing process are relieved either by heating or longer compression times when not heated. The material shows a discernible shift in its physical properties upon compression at 200°C. Initially, the material exhibits a nearly linear response, followed by the onset of viscous flow under a consistent stress level.

## 6 Summary and Conclusion

Seals made of elastomer are often unsuitable for sealing rotating shafts in thermally or chemically challenging conditions. In contrast, sleeve type lip seals are employed in this area of application. Unlike rotary shaft seals made of elastomer, sleeve type lip seals do not form a self-induced back-pumping effect that enables continuous operation without leakage. In order to achieve an optimum combination of chemical and thermal resistance, as well as static and dynamic tightness, a sleeve type lip seal with special back-pumping structures, designated the B3S, was developed at the IMA. To test the functional principle, the prototypes have so far been produced using laser engraving. However, this process is very time-consuming and involves problematic emissions during production. The studies presented in this paper have demonstrated that stamping is an optimal manufacturing process for back-structured shaft seals. This implies that a simpler, more efficient manufacturing process is now available that is associated with fewer harmful emissions. Stamping creates additional active back-pumping structures on the contact side, thus resulting in an enhanced back-pumping effect compared to the variant produced by laser engraving. The back-pumping effect can be significantly influenced by the stamping pressure and temperature.

## 7 Outlook

The data obtained from the material analysis now permits the precise design of the stamped structures through the use of simulative optimization. The effects of the stamping process can now be incorporated into the design. Furthermore, the test results can be used to optimize the pumping effect and to develop a B3S with optimized stamped bidirectional pumping structures.

## 8 References

[1] Patent EP 3555503 B1, Device for Sealing an Object, 2021

[2] Müller, H. K.; Nau B. S.: *Fluid Sealing Technology : Principles and Applications*. New York : Dekker, 1998

[3] Nakamura, K.; Kawahara, Y.: *An Investigation of Sealing Properties of Lip Seals through Observation of Sealing Surfaces under Dynamic Conditions*. 10th International Conference on Fluid Sealing, BHRA The Fluid Engineering Centre, Cranfield, Bedford, England, 1984

[4] Bauer, F.: *Federvorgespannte-Elastomer-Radial-Wellendichtungen. Grundlagen der Tribologie & Dichtungstechnik, Funktion und Schadensanalyse*. Springer Vieweg, Wiesbaden, 2021, ISBN 978-3-658-32921-1

[5] Schmitt, W.: *Radial Shaft Seal with PTFE Sealing Lips*. SAE Technical Paper 852347, 1985

[6] Gölz, J.: *Manschettendichtringe aus PTFE-Compounds – Funktionsmechanismus von PTFE-Manschettendichtungen und Entwicklung von Rückförderstrukturen für beidseitig drehende Wellen*. Dissertation, University of Stuttgart, 2017

[7] Bauer, F.: *PTFE-Manschettendichtungen mit Spiralrille – Analyse, Funktionsweise und Erweiterung der Einsatzgrenzen*. Dissertation, University of Stuttgart, 2008

[8] Stoll, M.; Dakov, N.; Hörl, L.; Bauer, F.: *A New Innovative Design for Shaft Seals*. 24th International Conference on Fluid Sealing, BHR Group, Manchester, 2018, P. 119-131, ISBN: 978-1-85598-1638

[9] Chiad, M.; Fatu, A.; Hajjam, M.: *Experimental study of PTFE lip seals with spiral grooves*. 21st International Conference on Fluid Sealing, BHR Group, Milton Keynes, UK, 2011

[10] Hoffmann, C.: *Untersuchungen an PTFE-Wellendichtungen*. Dissertation, University of Stuttgart, 1995

[11] Patent EP 0128645 A2, *Bi-directional hydrodynamic seal*. 1984

[12] Stoll, M.: *Entwicklung und Funktionsanalyse rückenstrukturierter Manschettendichtringe aus PTFE-Compound*. Dissertation, University of Stuttgart, 2019, ISBN 978-3-936100-93-8

[13] Garlock GmbH: *Garlock_GSK_3-1_Gasketing_Technical_Manual*. 03.2017

[14] Feldmeth, S.; Stoll, M.; Bauer, F.: *How to measure the radial load of radial lip seals*. Tribologie + Schmierungstechnik, 68. Jahrgang 3-4/2021

[15] Institut für Maschinenelemente: *TechSheet #102070 – Sealobserver*. University of Stuttgart, 2019

## 9 Authors

**University of Stuttgart, Institute of Machine Components (IMA)**
**Pfaffenwaldring 9, 70569 Stuttgart, Germany:**

Marco Gohs, M. Sc., ORCID 0000-0003-4747-6738,
marco.gohs@ima.uni-stuttgart.de

Dipl. Ing. Lothar Hörl, ORCID 0000-0002-2851-3364,
lothar.hoerl@ima.uni-stuttgart.de

Prof. Dr.-Ing. Frank Bauer, ORCID 0000-0001-7799-7628,
frank.bauer@ima.uni-stuttgart.de

https://doi.org/10.61319/EFNFS9KB